Setup tuning using Lambda and anti-Lambda particles
DIRAC NOTE 2013-03

A. Benelli , V. Yazkov

September 20, 2013

1 Introduction

In order to check the general geometry of the DIRAC experiment, we use the Λ and $\bar{\Lambda}$ particles that decay in our setup into $p\pi^-$ and $\pi^+\bar{p}$. The Lambda mass is very well determined [1] and comparing the value reconstructed in our data with the published one we can be confident that our geometrical description is correct. The main factors that can influence the value of the Lambda mass are: the position of the Aluminum membrane and the opening angle of the two downstream arms, they will be discussed in this note in section 3.

The width of the Lambda mass distribution is another tool that we use to evaluate the resolution of the momentum reconstruction of the particles. There are several factors that can contribute to the momentum reconstruction resolution. The most important are: the multiple scattering in the Aluminum membrane and in the Drift Chambers (DC), the resolution of the DC planes, the alignment of the DC downstream and the multiple scattering in the upstream detectors. In order to evaluate the last one we have used the $\pi\pi$ data. Using the $\pi^+\pi^-$ vertex distribution at the target for experimental data and simulated data [2] the upstream multiple scattering has been quantified, and, since then, all the simulated data were generated taking into account these new measurements. Once fixed the upstream multiple scattering we attribute the remaining difference between experimental and simulated data to the DC "effect" on the track reconstruction. Once corrected for this effect, we obtain an evaluation of the momentum resolution in a momentum range larger that the one used with the $\pi^+\pi^-$ pair analysis.

This study has been already performed in the past on the previous experimental setup and many notes were published on the subject [3].

2 Event selection

We select Λ and $\bar{\Lambda}$ particle events from the experimental data 2008, 2009 and 2010 that have been collected using a dedicated trigger. The following cuts are applied :

- in prompt events, the time difference in the vertical hodoscope (VH) is $|\Delta T_{VH}| < 0.5ns$
- the transverse momentum between pion and proton $Q_T < 10$ MeV/c
- to avoid mis-matching in the reconstruction, pion and proton tracks should be separated in at least two planes of the SFD detector, then two of the following criteria on the distance of the

hit columns, Δn_{SFD}, associated to the tracks should be true :$|\Delta n_{SFDx}| > 5$, $|\Delta n_{SFDy}| > 5$, $|\Delta n_{SFDw}| > 7$

- in order to take into account any difference between the distributions of the generated momenta for the simulated Lambda particles and the experimental one, we apply a weight on the MC events to correct for this effect
- we have generated Lambda and anti-Lambda events using the last results we have on the multiple scattering in the SFD detector [2]

The simulated data have been submitted to the same selection cuts.

3 Lambda mass

The study has been performed on the experimental data for the years 2008, 2009 and 2010. For every year data-set we have used the appropriate corresponding simulation, the different calibration of the detectors, and the different conditions of background.

Following what has been already done in the past [3], looking at the Lambda mass value after changing the geometrical parameters, we have verified that the position of the Aluminum membrane and the opening angle of the downstream arms are correctly evaluated. As a first approximation the best value for z coordinate of the Aluminum membrane from the center of the magnet is:

$$PosMembrane = 143.385 \text{ cm}$$

this value is then used during the tracking procedure as the z coordinate of the track in the exit plane of the magnetic field of the spectrometer magnet.

The opening angle of the DC arms (in the X-plane) should be corrected by the quantity

$$TgxDC = (-0.10 \quad 0.10)\ 10^{-3}\text{radian}$$

This means that the downstream arms axes are 0.10 milliradian wider that the default GEANT description of the experiment, in a symmetric way.

Fig 1 shows the distribution of the Lambda and anti-Lambda masses for the 2008, 2009 and 2010 data run, the distributions are fitted by ROOT with a gaussian and a second degree polynomial, that describes the background, the results are given for $\Lambda - 1.11\text{GeV/c}^2$ and $\bar{\Lambda} - 1.11\text{GeV/c}^2$ in Table 1.

Λ mass - 1.11 GeV/c^2	Data	MC
2008	$5.661\ 10^{-3} \pm 2.6\ 10^{-6}$	$5.680\ 10^{-3} \pm 1.0\ 10^{-6}$
2009	$5.680\ 10^{-3} \pm 2.3\ 10^{-6}$	$5.670\ 10^{-3} \pm 1.0\ 10^{-6}$
2010	$5.675\ 10^{-3} \pm 2.82\ 10^{-6}$	$5.65\ 10^{-3} \pm 1.0\ 10^{-6}$
anti-Λ mass - 1.11 GeV/c^2	Data	MC
2008	$5.75\ 10^{-3} \pm 1.7\ 10^{-5}$	$5.63\ 10^{-3} \pm 1.2\ 10^{-6}$
2009	$5.73\ 10^{-3} \pm 1.7\ 10^{-5}$	$5.73\ 10^{-3} \pm 1.8\ 10^{-6}$
2010	$5.73\ 10^{-3} \pm 2.1\ 10^{-5}$	$5.67\ 10^{-3} \pm 1.2\ 10^{-6}$

Table 1: Lambda mass in GeV/c^2 for the 2008, 2009 and 2010 experimental and MC data.

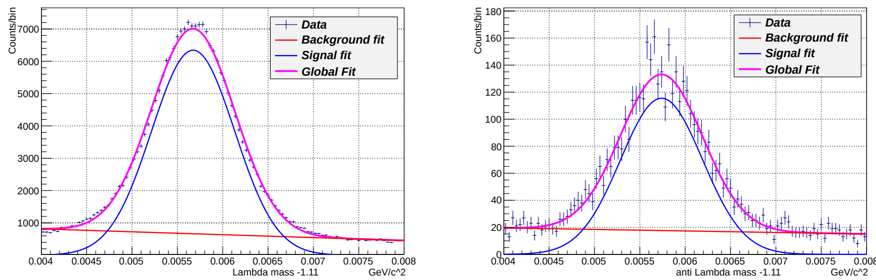

Figure 1: Lambda and anti-Lambda mass distributions for the 2008 experimental data.

Λ width -1.11 GeV/c^2	Data	MC
2008	$4.62\ 10^{-4} \pm 1.8\ 10^{-6}$	$4.18\ 10^{-4} \pm 1.1\ 10^{-6}$
2009	$4.57\ 10^{-4} \pm 2.4\ 10^{-6}$	$4.22\ 10^{-4} \pm 1.1\ 10^{-6}$
2010	$4.56\ 10^{-4} \pm 1.4\ 10^{-6}$	$4.36\ 10^{-4} \pm 1.1\ 10^{-6}$
anti-Λ width -1.11 GeV/c^2	Data	MC
2008	$4.59\ 10^{-4} \pm 1.8\ 10^{-5}$	$4.30\ 10^{-4} \pm 1.3\ 10^{-6}$
2009	$4.34\ 10^{-4} \pm 1.7\ 10^{-5}$	$4.30\ 10^{-4} \pm 1.3\ 10^{-6}$
2010	$4.58\ 10^{-4} \pm 2.0\ 10^{-5}$	$4.25\ 10^{-4} \pm 1.3\ 10^{-6}$

Table 2: Lambda width in GeV/c^2 for the 2008, 2009 and 2010 experimental and MC data.

The weighted average of the Dirac experimental value for the Λ and $\bar{\Lambda}$ particles masses

$$\text{Mass } \Lambda_{\text{Dirac}} = 1.115685 \pm 1.2\ 10^{-6}\text{GeV/c}^2$$

for the entire set of data of 2008, 2009 and 2010, in very good agreement with the PDG value

$$\text{Mass } \Lambda_{\text{PDG}} = 1.115683 \pm 6\ 10^{-6}\text{GeV/c}^2$$

This confirms that the geometry of the Dirac experiment is well described.

The anti-Lambda mass is larger than the PDG value by 1%, for the sum of the 2008, 2009 and 2010 data, $\bar{\Lambda} = 1.11573 \pm 1.1\ 10^{-5}\text{GeV/c}^2$. In order to have a feeling of how much is important for DIRAC the difference in the mass values found for Lambda and anti-Lambda particles we have reconstructed $\Lambda(\bar{\Lambda})$ events as if they were $\text{K}^-\pi^+(\text{K}^+\pi^-)$ events. Lambda particles imitate $\text{K}^+\pi^-$, the proton (heavier particle) in the pair has positive charge as the K^+ and can fake the kaon in the analysis. Correspondingly, anti-Lambda imitates $\text{K}^-\pi^+$. The Q_l distribution is centred for the "anti-Lambda" events in $Q_l^{\text{K}^-\pi^+} = 31.09 \pm 0.013\text{MeV/c}$ and for the "Lambda" events in $Q_l^{\text{K}^+\pi^-} = -30.8 \pm 0.00014\text{MeV/c}$ [Figure 2], giving us a shift with respect to the complete symmetry of 0.27 MeV/c. This does not represent a problem for the Data Analysis since the Ql resolutions for the Kπ channel and $\pi\pi$ are larger [4].

In order to check if there are hidden effects for a particular momentum of the particles we have divided our sample in three momentum ranges depending on the momenta of the p and π^-. Increasing the momentum of the pπ^- we see that the width of the distribution increases, as is

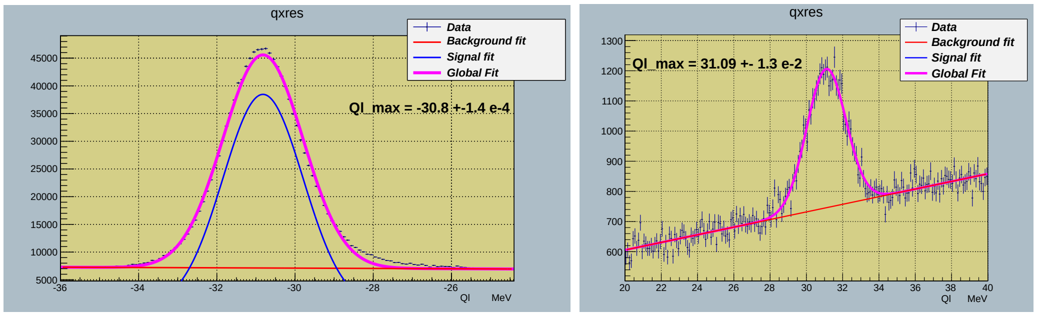

Figure 2: Ql distribution of Lambda and anti-Lambda events reconstructed as Kπ events.

expected because the contribution of the DC resolution to the momentum reconstruction error increases with the increase of the momentum. No particular effect is seen for any momentum range on the mass value comparing the results that are shown in Table 3 for the experimental data and in Table 4 for the simulated data.

Λ width -1.11 GeV/c^2	2008	2009	2010
$p_{\rm p} + p_{\pi^-} < 5.8$GeV/c	$M = 5.66\ 10^{-3} \pm 5.\ 10^{-6}$ $\sigma = 4.29\ 10^{-4} \pm 6.\ 10^{-6}$	$M = 5.66\ 10^{-3} \pm 4.\ 10^{-6}$ $\sigma = 4.25\ 10^{-4} \pm 4.\ 10^{-6}$	$M = 5.66\ 10^{-3} \pm 3.\ 10^{-6}$ $\sigma = 4.27\ 10^{-4} \pm 4.\ 10^{-6}$
$5.8 < p_{\rm p} + p_{\pi^-} < 7.$GeV/c	$M = 5.65\ 10^{-3} \pm 4.\ 10^{-6}$ $\sigma = 4.44\ 10^{-4} \pm 5.\ 10^{-6}$	$M = 5.67\ 10^{-3} \pm 3.\ 10^{-6}$ $\sigma = 4.45\ 10^{-4} \pm 4.\ 10^{-6}$	$M = 5.67\ 10^{-3} \pm 3.\ 10^{-6}$ $\sigma = 4.39\ 10^{-4} \pm 4.\ 10^{-6}$
$p_{\rm p} + p_{\pi^-} > 7.$GeV/c	$M = 5.66\ 10^{-3} \pm 5.\ 10^{-6}$ $\sigma = 4.73\ 10^{-4} \pm 7.\ 10^{-6}$	$M = 5.69\ 10^{-3} \pm 5.\ 10^{-6}$ $\sigma = 4.79\ 10^{-4} \pm 6.\ 10^{-6}$	$M = 5.68\ 10^{-3} \pm 5.\ 10^{-6}$ $\sigma = 4.68\ 10^{-4} \pm 6.\ 10^{-6}$

Table 3: Experimental Lambda mass (M) and width (σ) for different momentum bins.

Λ width -1.11 GeV	2008	2009	2010
$p_{\rm p} + p_{\pi^-} < 5.8$GeV/c	$M = 5.67\ 10^{-3} \pm 5.\ 10^{-6}$ $\sigma = 4.06\ 10^{-4} \pm 4.\ 10^{-6}$	$M = 5.67\ 10^{-3} \pm 4.\ 10^{-6}$ $\sigma = 4.09\ 10^{-4} \pm 4.\ 10^{-6}$	$M = 5.65\ 10^{-3} \pm 4.\ 10^{-6}$ $\sigma = 4.14\ 10^{-4} \pm 4.\ 10^{-6}$
$5.8 < p_{\rm p} + p_{\pi^-} < 7.$GeV/c	$M = 5.67\ 10^{-3} \pm 4.\ 10^{-6}$ $\sigma = 4.23\ 10^{-4} \pm 6.\ 10^{-6}$	$M = 5.67\ 10^{-3} \pm 5.\ 10^{-6}$ $\sigma = 4.21\ 10^{-4} \pm 5.\ 10^{-6}$	$M = 5.64\ 10^{-3} \pm 5.\ 10^{-6}$ $\sigma = 4.23\ 10^{-4} \pm 6.\ 10^{-6}$
$p_{\rm p} + p_{\pi^-} > 7.$GeV/c	$M = 5.62\ 10^{-3} \pm 6.\ 10^{-6}$ $\sigma = 4.22\ 10^{-4} \pm 6.\ 10^{-6}$	$M = 5.64\ 10^{-3} \pm 6.\ 10^{-6}$ $\sigma = 4.38\ 10^{-4} \pm 6.\ 10^{-6}$	$M = 5.62\ 10^{-3} \pm 6.\ 10^{-6}$ $\sigma = 4.37\ 10^{-4} \pm 6.\ 10^{-6}$

Table 4: Simulated Lambda mass (M) and width (σ) for different momentum bins.

4 Lambda mass width

The width of the Lambda mass distribution is a test of how well we reproduce the data in the simulation. From both the Tables 3 and 4 we see a consistent underestimation of $6-7\%$ between the Lambda width in the simulation and in the experimental data.

This effect is the consequence of the imperfect description of the downstream part of the detector and can be fixed introducing a gaussian smearing in the reconstructed momenta. We apply event by event the smearing given by the formulae below where $p(\mathrm{p})$ and $p(\pi^-)$ are the reconstructed proton and pion momenta respectively, and Gauss(0,0.0001) is a random number generated accordingly to a Gaussian distribution with mean = 0 and sigma=0.0001.

$$p(\mathrm{p})^{smeared} = p(\mathrm{p})\ (1 + j \times Gauss(0, 0.0001))$$

$$p(\pi^-)^{smeared} = p(\pi^-)\ (1 + j \times Gauss(0, 0.0001))$$

We let j vary between 0 and 20, and for every value of j we build a new Lambda mass distribution. We then compare (bin by bin) the experimental and MC distributions building a Chi^2 distribution using the following formulae

$$Chi^2 = \Sigma_i \frac{(Data(i) - Mc_j(i))^2}{(\sigma^2_{Data(i)} + \sigma^2_{MC(i)})}$$

see Figure 3. The simulated distribution has been normalised to the Experimental number of events. Fitting with an additional second degree polynomial we can find the minimum of the distribution for $j = 7 \pm 4$.

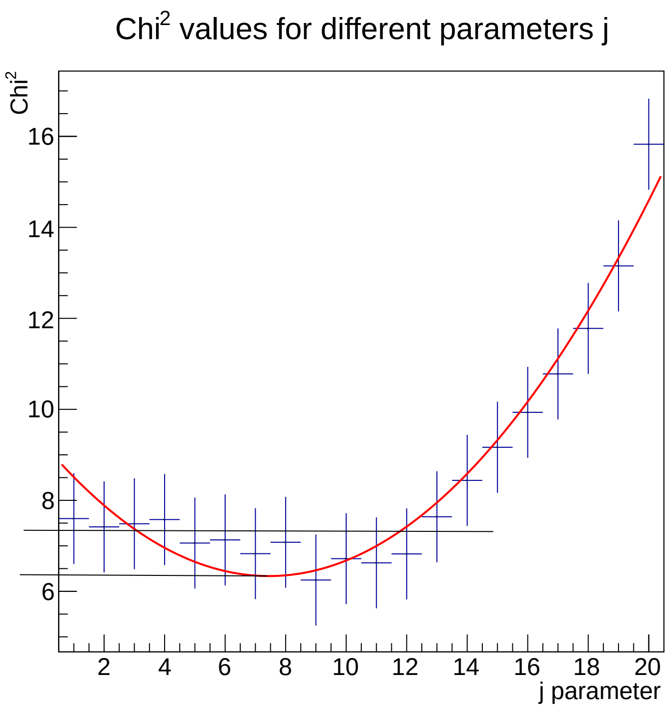

Figure 3: Chi^2 distribution for different values of the parameter j.

We then apply the smearing of 0.0007 to the reconstructed momenta, and as expected the data and simulated distributions are in perfect agreement, Fig 4.

5 Final checks and momentum resolution

The Ql distribution of the $\pi^+\pi^-$ can be used as a test for checking the geometrical alignment. Since the $\pi^+\pi^-$ system is symmetric the corresponding Ql distribution should be centred in 0. Fig 5 shows the experimental distribution of the longitudinal momentum of the pions-pair for transverse momenta $Q_T < 4$ MeV/c, the distribution is centred at 0 with a precision of 0.2 MeV/c.

Taking now into account the momentum smearing we can evaluate the momentum resolution for our detector as $\frac{dp}{p} = \frac{p_{gen} - prec}{p_{gen}}$ where p_{gen} and p_{rec} are the generated and reconstructed momenta respectively.

Λ particles are used as well to test the momentum resolution. MonteCarlo simulation distributions are presented in Fig . 6 , giving us the confidence that our spectrometer is able to reconstruct with a relative precision between 2.8 10^{-3} and 4.4 10^{-3} for particles with momenta between 1.5 and 8 GeV/c.

References

[1] The Review of Particle Physics J. Beringer et al. (Particle Data Group), Phys. Rev. D86, 010001 (2012)

[2] DIRAC-NOTE-2012-04 , Multiple scattering studies, A. Benelli [JINR, Zurich] and V. Yazkov [SINP, Moscow]

[3] DIRAC-NOTE-2009-10, The alignment of DIRAC setup for year 2008 using the properties of Lambda peak and ΔX coordinate at the target distributions, O. Gortchakov [JINR] ; DIRAC-NOTE-2009-08, The new results on the Lambda peak width and ΔX coordinates at the target for 2002 year and comparison with MC results, O. Gortchakov [JINR] ; DIRAC-NOTE-2009-02, The new results on the Lambda peak width for data samples at different years and comparison with MC results, O. Gortchakov [JINR] ; DIRAC-NOTE-2008-09, The Lambda peak width for data samples at different years, comparison with MC results, O. Gortchakov [JINR] ; DIRAC-NOTE-2005-16 Study of multiple scattering in upstream detectors in DIRAC, B. Adeva, A. Romero, O. Vazquez Doce [Santiago].

[4] Detection of atoms with the DIRAC spectrometer at CERN, J. Phys. G: Nucl. Part. Phys. 30 (2004) 1929-1946.

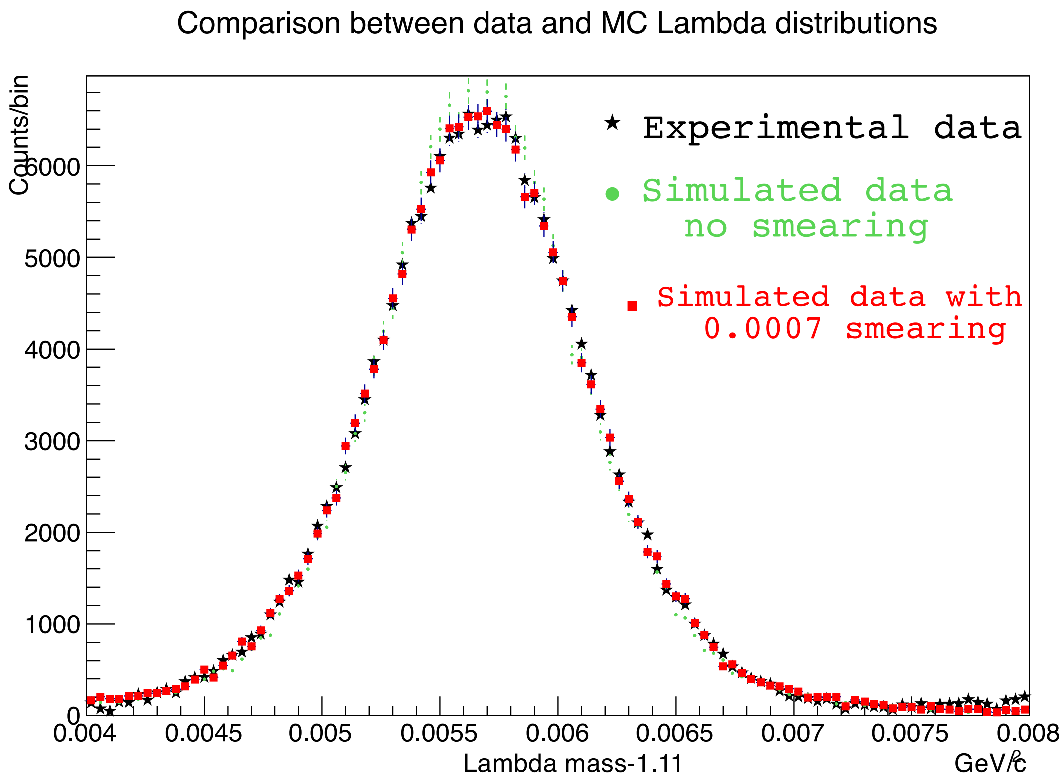

Figure 4: Lambda MC and experimental data superimposed, in green is the MC distribution with no smearing applied, in red is the MC simulation with the smearing of 0.0007 applied, in black is the experimental data distribution.

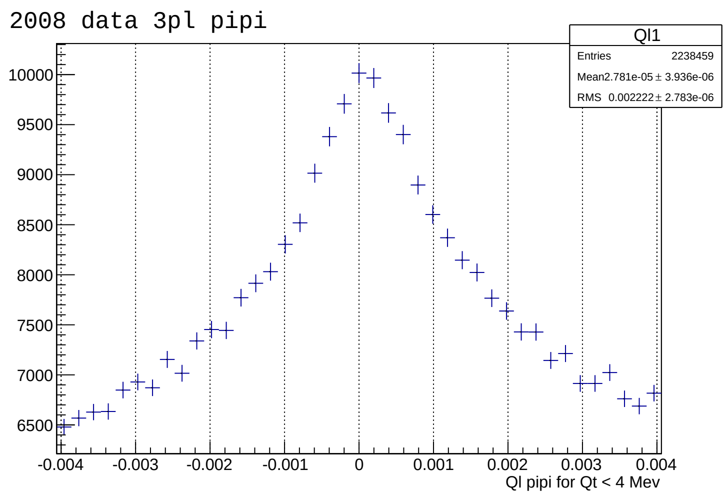

Figure 5: Ql distribution for $\pi^+\pi^-$ experimental data.

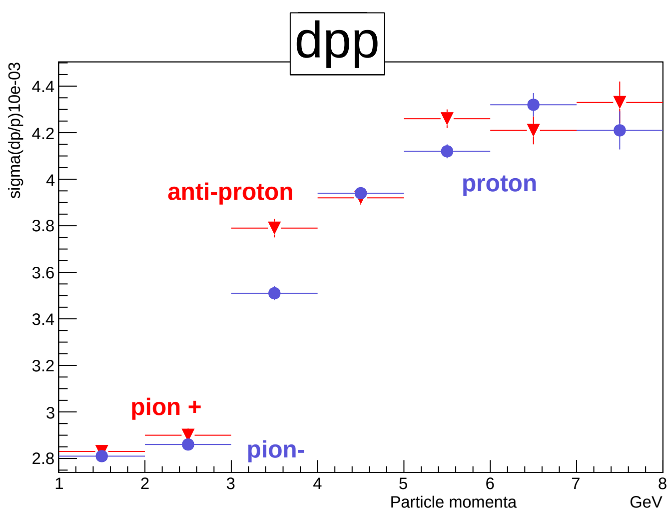

Figure 6: Momentum resolution